MINIMUM VERTICAL REINFORCEMENT IN DUCTILE REINFORCED CONCRETE WALLS

Y. Lu[(1)] and R.S. Henry[(2)]

[(1)] *PhD candidate, University of Auckland, lyqhnu@gmail.com*
[(2)] *Senior Lecturer, University of Auckland, rs.henry@auckland.ac.nz*

Abstract

Research into the seismic design of lightly reinforced concrete (RC) walls was initiated following the Canterbury earthquakes in New Zealand when several walls were observed to have formed only a limited number of cracks in the plastic hinge region. Initial investigation highlighted that vertical reinforcement content and distribution were critical parameters that influenced the ductility of lightly reinforced concrete walls. A total of ten half scale walls were tested to investigate the seismic behaviour of multi-story RC walls with minimum vertical reinforcement. Six walls were designed with minimum required distributed vertical reinforcement in accordance with existing New Zealand Concrete Structures Standard (NZS 3101:2006). An additional four test walls were designed with additional vertical reinforcement in the ends of the walls, as is required by some design standards and proposed amendments for ductile RC walls in NZS 3101:2006 (A3 draft). The experimental results of three of these test walls are presented and discussed. The test results indicated that typical minimum distributed vertical reinforcement requirements, such as those in NZS 3101:2006 (A2), were insufficient to ensure that a large number of secondary cracks formed, and are only suitable for walls designed for low ductility demands. Additionally, the concentration of inelastic reinforcement strains at wide cracks resulted in premature reinforcement buckling even when closely spaced transverse reinforcement was used. The RC walls tested with a small amount of additional vertical reinforcement in the ends of the wall displayed significantly greater crack distribution in the plastic hinge region and more evenly distributed reinforcement strains. The test results and analysis have been used to provide recommendations for suitable minimum vertical reinforcement provisions for walls with a range of ductility demands.

Keywords: seismic design, reinforced concrete walls; vertical reinforcement, minimum requirement, plastic hinge region.

1. Introduction

Reinforced concrete (RC) walls are commonly used as lateral force resisting elements in both low-rise and high-rise buildings. Ductile RC walls resist lateral forces imposed on the structure during earthquakes through the formation of a flexural plastic hinge at the wall base. The ductility and deformation capacity in the plastic hinge region results from the inelastic action of cracking and crushing of concrete and yielding of vertical (longitudinal) reinforcement. The rotational capacity of the plastic hinge is dependent on the distribution of cracking, with a greater number of flexural cracks allowing the vertical reinforcement to yield over a significant length. Therefore to achieve good ductility during earthquakes, RC walls should be designed to form a large number of distributed primary and secondary flexural cracks in the plastic hinge region.

During the 2010/2011 Canterbury earthquakes in New Zealand, several lightly reinforced concrete walls in multi-story buildings formed a limited number of cracks in the plastic hinge region as opposed to the expected distributed cracking [1-3]. Because of the lack of distributed cracks, the inelastic deformation concentrated over a short plastic hinge length, resulting in premature fracture of vertical reinforcement. Examples of RC walls with limited cracks following the Canterbury Earthquakes are shown in Fig. 1. In response to the observed performance of lightly reinforced concrete walls, the Canterbury Earthquakes Royal Commission (CERC) highlighted the need for further research to ensure yielding of reinforcement can extend over a significant height of the wall rather than just the immediate vicinity of a limited number of primary cracks.

(c) Limited cracking
(Credit: Charles Clifton)

(c) Limited cracking and reinforcement buckling
(Credit: Ken Elwood)

(d) Fractured bars
(Credit: Des Bull)

Fig. 1 - Examples of observed damage to lightly reinforced concrete walls

Minimum reinforcement requirements for RC walls are imposed by most concrete design standards worldwide, both to mitigate shrinkage and temperature effects, and to prevent non-ductile failure modes. If insufficient vertical reinforcement is provided in RC walls, the cracking moment may exceed the nominal moment capacity of the wall and sudden loss of strength and failure may occur. Additionally, for walls designed to exhibit ductility during earthquakes, the tension force generated by the reinforcement may not be sufficient to develop secondary flexural cracks in the surrounding concrete, resulting in a limited number of cracks and limited ductility [4].

Most concrete design standards require at least 0.12% vertical (or longitudinal) reinforcement in all RC walls, which is in line with temperature and shrinkage requirements. For seismic resisting walls, a higher minimum distributed vertical reinforcement content is usually required, equal to 0.15 or 0.25% in ACI 318-14 [5], 0.20% in Eurocode 8 [6] and 0.25% in CSA A23.3-14 [7] and GB 50010-2010 [8]. The New Zealand Concrete Structures Standard, NZS 3101:2006 [9], requires minimum distributed vertical reinforcement that depends on both the concrete and reinforcement strength, and typically ranges from 0.25-0.70%. For RC walls designed to exhibit ductility during earthquakes, some standards such as Eurocode 8, GB 50010-2010, and CSA A23.3-14, require additional vertical reinforcement to be concentrated in the ends of the walls. Recently, new amendments have been proposed to the minimum vertical reinforcement requirements for ductile RC walls in NZS 3101:2006 (A3 draft) [10], which also requires additional minimum vertical reinforcement in the wall end zone. The

proposed limits for NZS 3101:2006 (A3 draft) were developed based on the development of distributed secondary cracks in the plastic hinge region [11].

To investigate the seismic behaviour of multi-story RC walls with only minimum distributed vertical reinforcement, and walls with additional reinforcement concentrated in the ends of the wall, a total of ten half scaled test walls were tested. Six walls were designed with minimum distributed vertical reinforcement in accordance with the existing NZS 3101:2006 (A2) and an additional four test walls were designed in accordance with the proposed amendments to minimum vertical reinforcement requirements for ductile RC walls in NZS 3101:2006 (A3 draft). The experimental results of three typical test walls are presented that highlight the key differences between the test walls and minimum vertical reinforcement requirements.

2. Experimental Investigation

2.1 Test walls

Ten large-scale RC cantilever test walls were constructed and subjected to pseudo-static reverse cyclic loading. A summary of the ten test walls is shown in Table 1, and drawings of the cross sections of the wall specimens are shown in Fig. 2. The 1.4 m long, 2.8 m high and 150 mm thick wall specimens were designed to approximately represent the lower portion of a 40-50% scale wall in a multi-storey building.

Table 1 - Details of the RC test walls

Wall	Shear span ratio	Axial load ratio	Material properties		Vertical reinforcement ratio (%)			Horizontal reinforcement ratio (%)	End stirrups (mm)
			f_c' (MPa)	f_y (MPa)	End region	Web region	Total		
C1	2	3.5%	30	300		0.47	0.53	0.25	No
C2	4	3.5%	30	300		0.47	0.53	0.25	No
C3	6	3.5%	30	300		0.47	0.53	0.25	No
C4	2	0	30	300		0.47	0.53	0.25	No
C5	2	7%	30	300		0.47	0.53	0.25	D6@90
C6	4	3.5%	30	300		0.47	0.53	0.25	D6@60
M1	4	3.5%	30	300	1.00	0.47	0.67	0.25	D6@60
M2	4	3.5%	30	300	1.44	0.47	0.80	0.25	D6@60
M3	4	3.5%	30	300	0.72	0.47	0.59	0.25	D6@60
M4	4	3.5%	30	300	1.28	0.47	0.76	0.25	D6@60

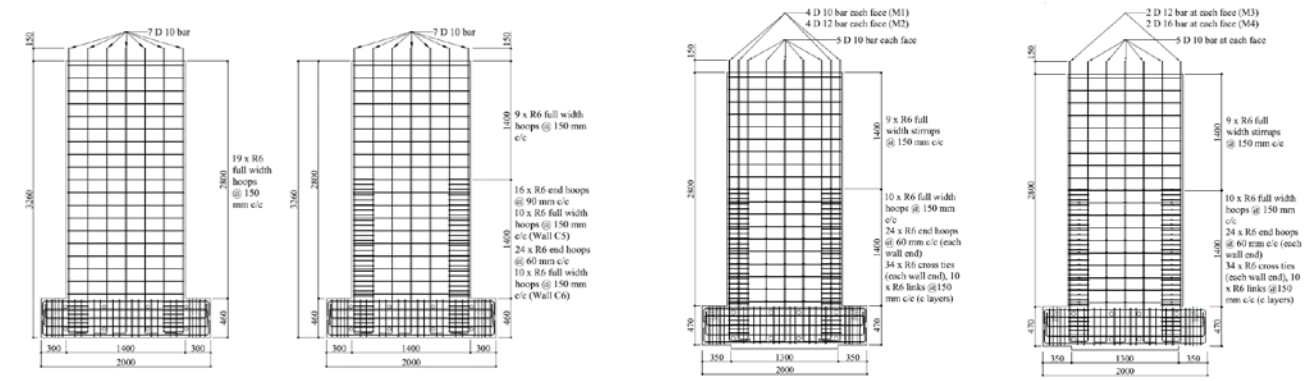

(a) Evaluation

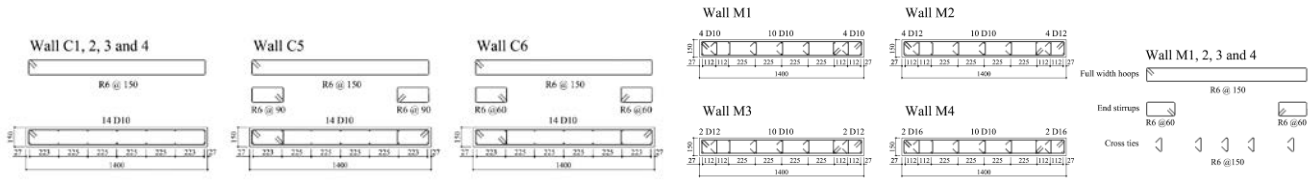

(b) Sections

Fig. 2 - Details of test walls

As shown in Table 1, the first phase included six walls (C1-C6) that were designed with limited ductility as per NZS 3101:2006 (A2). The vertical reinforcement was identical for all six walls and distributed evenly to satisfy the minimum requirements for vertical reinforcement in NZS 3101:2006 (A2), and shown in Eq. 1.

$$\rho_l \geq \sqrt{f_c'} \Big/ \left(4 f_y\right) \tag{1}$$

It should be noted that the resulting distributed vertical reinforcement ratio of 0.47% in walls C1-C6 is larger than that required by other design standards that only requires a fixed minimum distributed vertical reinforcement. For example, ACI 318-14 [5] would require only 0.15% for the test wall. Three shear span ratios of 2, 4, and 6 were applied to the test walls to represent walls in a range of different building heights. The applied axial load was also varied from 0-7% of the wall axial capacity. The axial load for wall C5 triggered the NZS 3101:2006 requirement for additional confinement reinforcement in the ends of the wall to achieve a limited ductile response. Wall C6 was identical with Wall C2 expect that stirrups to provide anti-buckling restraint were added in the ends of the wall.

The second phase included four walls (M1-M4) designed for a ductile response in accordance with proposed provisions in NZS 3101:2006 (A3 draft). In addition to distributed minimum vertical reinforcement in the central web region of the wall of 0.46% in accordance with Eq. 1, NZS 3101:2006 (A3 draft) also requires additional vertical reinforcement in the ends of the wall as per Eq. 2, where ρ_{le} is the end zone reinforcement ratio applied over a length of $0.15l_w$.

$$\rho_{le} \geq \sqrt{f_c'} \Big/ \left(2 f_y\right) \tag{2}$$

As shown in Fig. 2, walls M1-M4 were comparable to that tested in the first phase, expect that the vertical reinforcement ratio in the end zone was varied from 0.72% to 1.44%. Wall M1 was designed to closely satisfy the proposed new minimum vertical reinforcement requirements which had an end zone reinforcement ratio of 1.0%, resulting in four D10 placed at ends of the wall. The end zone vertical reinforcement ratio of wall M2 was 1.44%, consisting of four D12 bars, which was higher than the Eq. 2 requirement. Wall M3 did not satisfy the proposed minimum vertical reinforcement requirements in the ends of the wall, and was designed to investigate either a reduced end zone reinforcement ratio of 0.72%, or a smaller end zone length ($0.1l_w$). Wall M4 had a similar end zone vertical reinforcement ratio as wall M1, but used two D16 reinforcement bars instead of four D10 bars to investigate using larger diameter bars right in the ends of the wall. The minimum required end zone vertical reinforcement ratio 0.91% in NZS 3101:2006 (A3 draft) was slightly less than the 1.0% limit in the ends of ductile RC walls in CSA A23.3-14 but significantly larger than the 0.5% required by Eurocode 8.

2.2 Test setup

Because of height limitations in the structural test hall, a test setup was designed to simulate the expected seismic loading on the bottom two storeys of a 40-50% scaled wall from a multi-storey building. Based on an assumed lateral-load distribution, the moment, shear, and axial loads at the second storey height can be calculated. The test setup developed for the RC wall specimen is shown in Fig. 3. An actuator was attached between the steel loading beam and the strong wall to apply horizontal loads to the wall, and two additional actuators were attached vertically at each end of the wall to achieve the required moment and axial load at the top of the wall.

2.3 Instrumentation

The test walls' response was monitored using a dense array of instrumentation, as shown in Fig. 4. The horizontal displacement at the top of the wall was measured using two string-pot displacement gauges and the forces and displacements applied by each actuator were monitored using internal load cells and LVDTs. On one face of the wall, steel studs were embedded in the concrete during construction approximately 30 mm from the wall edges. Displacement gauges were attached to these studs to measure the local deformations of different sections of the wall. A total of 9 displacement gauges were placed at each edge up the height of the wall to monitor axial strains and curvatures. Shear deformations in the wall were measured using displacement gauges in "X" configurations over two panel regions, as shown in Fig. 4. To accurately capture the cracking at the wall

base, two rows of 5 displacement gauges were placed along the wall length and extending 300 mm up the wall height. Steel studs were also welded directly onto the corner vertical reinforcement that passed through recesses in the cover concrete to allow the average reinforcement strains to be measured using external displacement gauges over a 150 mm gauge length. Displacement gauges were also used to measure any potential vertical and horizontal slip at the wall-to-foundation, wall-to-loading beam, and foundation to strong-floor joints.

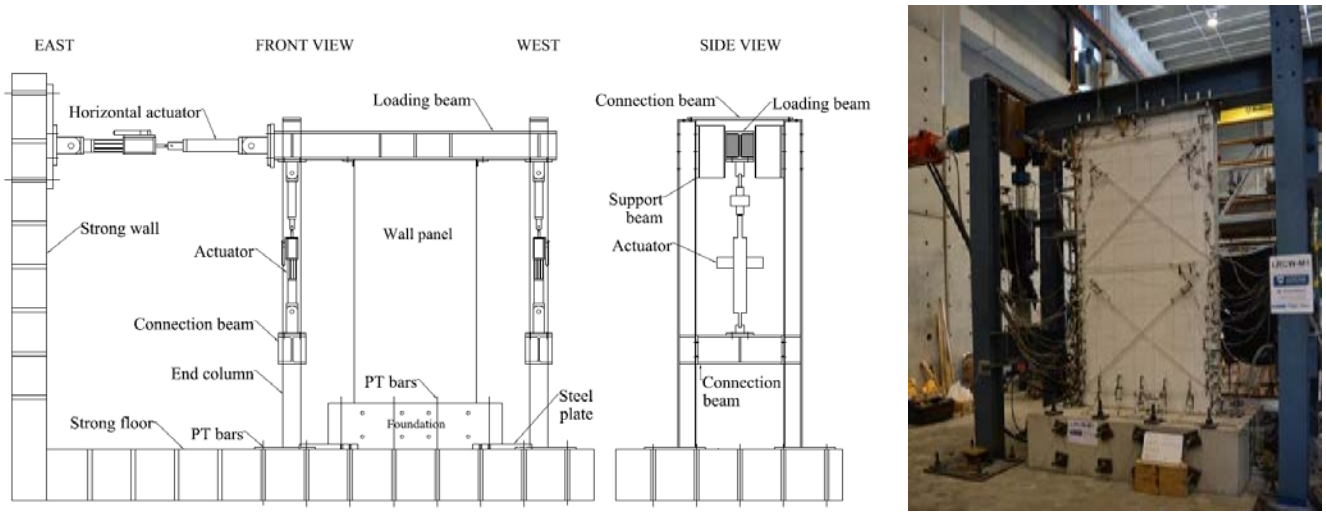

(a) Test setup illustration (b) Photo of test setup in lab

Fig. 3 - Test setup used to achieve the desired test moment to shear ratio

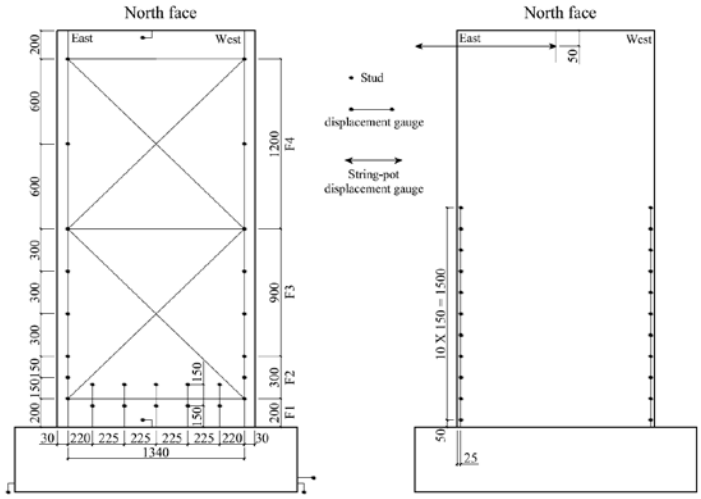

Fig. 4 - Instrumentation used for the test walls

3. Test observations and results

The experimental results of three test walls that were representative of the observed and measured behaviour are presented, consisting of wall C6, M1 and M2. These three test walls all had a shear span ratio of 4, axial load ratio of 3.5% and had D6 anti-buckling ties in wall toes at 60 mm centers. Table 2 provides a summary of the drift cycle during which key observations were made during the tests, including first cracking, concrete spalling, reinforcement buckling, core concrete crushing and reinforcement fracture. The crack patterns as well as the maximum measured crack widths at the end of the test of the three test walls are shown in Fig. 5. The final

condition of each of the walls is shown in Fig. 6 and the moment-displacement hysteresis response for all six test walls are shown in Fig. 7.

Table 2 - Key observations of all six test walls

Test wall	Direction	First cracking	Concrete spalling	Bar buckling	Core concrete crushing	Bar fracture
C6	+	+0.12%	+1.0%3	+1.5%3	N/A	+2.5%3
	-	-0.12%	-2.0%1	-2.0%3	N/A	-2.0%2
M1	+	N/A	+2.0%[1 a]	+2.0%[3]	+3.5%[3]	+2.5%[2]
	-	N/A	-2.0%[1]	-2.0%[2]	-3.5%[1]	-2.5%[3]
M2	+	+0.2%[1]	+2.0%[3]	+2.5%[3]	+3.5%[1 b]	+3.5%[1]
	-	-0.2%[1]	-2.0%[3]	-2.5%[2]	-3.5%[2]	-3.5%[3]

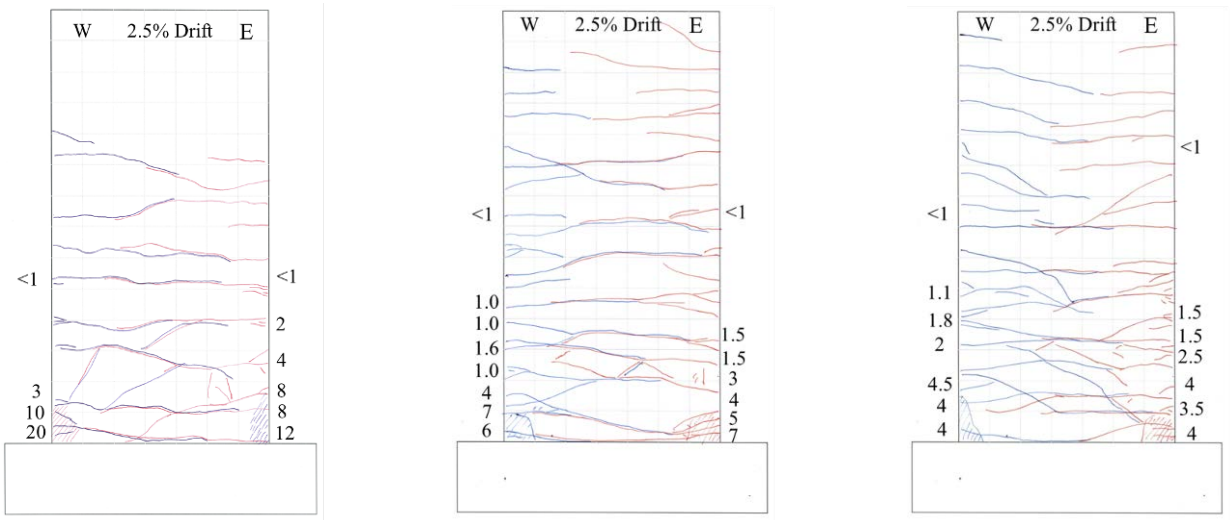

(a) Wall C6 (b) Wall M1 (c) Wall M2

Fig. 5 - Final crack patterns and maximum measured crack widths of the three test walls (mm)

(a) Wall C6 (b) Wall M1 (c) Wall M2

Fig. 6 - Photos of the wall toe at the end of each test

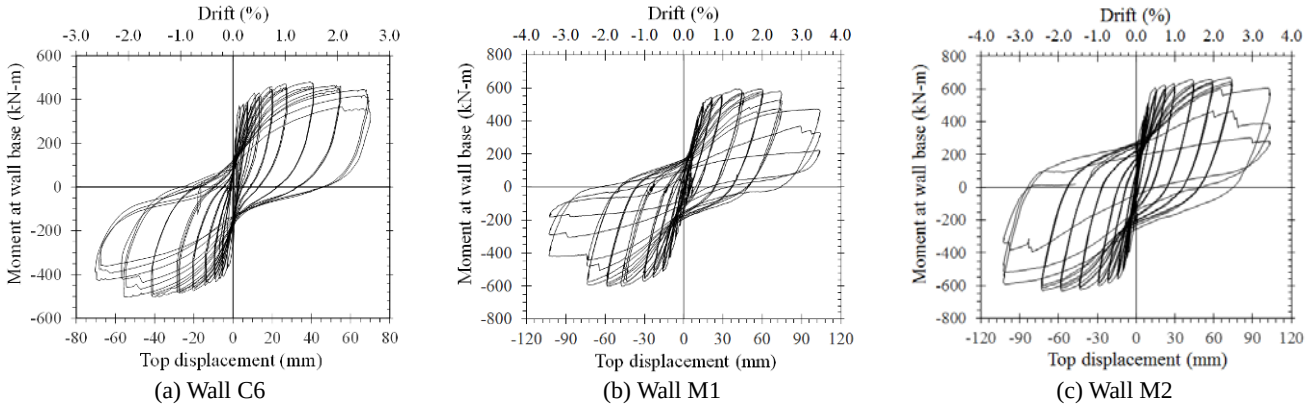

(a) Wall C6 (b) Wall M1 (c) Wall M2

Fig. 7 - Moment-displacement response for the three test walls

3.1 Wall C6

Test wall C6 was designed with distributed minimum vertical reinforcement ratio as per NZS 3101:2006 (A2) with no additional vertical reinforcement placed in the ends of the wall. As shown in Fig. 5-a, the wall response was dominated by 3-4 large flexural cracks at the wall base, with other cracks less than 2 mm wide. All the flexural cracks initiated prior to a lateral drift of ±0.5%, after which no significant new flexural cracks occurred during the test. During larger lateral drift cycles, the wall deformation was primarily concentrated at 1-2 large flexural cracks at the wall base which opened up to 20 mm wide with the other flexural cracks not opening wider than a few millimeters. Despite the presence of the anti-buckling reinforcement, the onset of concrete spalling and buckling of the vertical reinforcement was observed at the west end of the wall during a moderate drift of 1.5%. The two buckled reinforcing bars fractured during the second and third cycle to the drift of 2.0%, causing a large drop in lateral strength. Concrete spalling occurred at the east end of the wall during the first cycle to -2.0% lateral drift, but there was no sign of reinforcement buckling until the third cycle to -2.0% drift. The buckled reinforcing bar at the east end fractured during cycles to -2.5% lateral drift. The final condition at the west end of the wall is shown in Fig. 6-a.

As shown in Fig. 7-a, the uncracked wall had a high initial cross section stiffness and two flexural cracks initiated at a wall base moment of 334.9 kN-m, or roughly 70% of the peak strength. The strength started to drop during cycles to 1.5% lateral drift when the wall was pushed to west, while in other direction the wall maintained a stable response until -2.0% lateral drift when the reinforcement buckling occurred. The vertical reinforcing bars fracture during the first cycle to -2.5% lateral drift lead a 20% drop of peak strength. During the third cycle to lateral drift of +2.5%, the wall also experienced a large drop in strength due to fracture of additional vertical reinforcement along the wall length.

3.2 Wall M1

Wall M1 was identical with wall C6 except that wall M1 had additional pair of D10 reinforcement in the ends of the wall, resulting in an lumped vertical reinforcement ratio of 1.0%, which closely satisfies the minimum requirements proposed in NZS 3101:2006 (A3 draft). The wall response was dominated by flexural behaviour with a large number of horizontal cracks extending over almost the entire wall height. Compared to the test wall C6 that had minimum distributed reinforcement as per NZS 3101:2006 (A2), the cracks in wall M1 were more evenly distributed over the plastic hinge region. As shown in Fig. 5-b, wall M1 had more cracks and a smaller crack spacing compared to wall C6. The maximum crack width at drift of 2.5% was around 7 mm, which was significantly less than the large 20 mm crack width observed for wall C6 at the same drift level. Furthermore, unlike wall C6 in which all the flexural cracks formed prior to 0.5% lateral drift, new secondary cracks formed in wall M1 during cycles up to ±1.5% lateral drift. The cracking behaviour of wall M1 indicated that concentrating a greater portion of reinforcement in the ends of the wall can improve the crack distribution and control of crack widths.

Concrete spalling and reinforcement buckling in wall M1 were delayed when compared to wall C6 due to the even distribution of plasticity. The concrete at the corners of the wall started to spall and buckling of the vertical reinforcement initiated during cycles to lateral drifts of ±2.0%. The two buckled reinforcing bars at the east end fractured during the second and third cycle to +2.5% lateral drift, respectively. At west end, one reinforcing bar fractured during the third cycle to -2.5% lateral drift. Wall M1 was still in an acceptable condition after the cycles to 2.5% and so the wall was loaded to an additional cycle to 3.5% lateral drift. Subsequent reinforcing bar fracture occurred during the cycles to 3.5% lateral drift. The final condition on the east end of the wall is shown in Fig. 6-b.

As observed in the force-displacement response in Fig. 7-b, the initial cross section stiffness of wall M1 was slightly lower than expected due to unexpected cracking before the test when the vertical actuators were installed. However, the inelastic response was not effected and was stable up until 2.0% lateral drift when buckling of the vertical reinforcement caused strength degradation on subsequent cycle. A drop of 20% of the peak strength occurred when the buckled reinforcing bar fractured during the third cycle to +2.5% lateral drift.

3.3 Wall M2

Wall M2 was identical to wall M1 except that D12 bars replaced the D10 bars in the ends of the wall. resulting in a larger end region reinforcement ratio of 1.44%. Similar to wall M1, the behaviour of wall M2 was dominated by flexure with a large number of cracks occurring over the full wall height. As shown in Fig. 5-c, more obvious inclined shear cracks were observed in the central web region of the wall and slightly more secondary cracks occurred in the ends of the wall due to the larger lumped reinforcement ratio. New secondary cracks formed up until drift cycles to ±1.5%. In the later stages of the test, the inclined web cracks was wider than the cracks at wall edge due to the difference in the distributed reinforcement ratio in wall web and reinforcement ratio in the ends of the wall. Due to the stability of larger diameter reinforcing bars, concrete spalling and reinforcement buckling of wall M2 was delayed when compared to wall M1, and initiated during cycles to ±2.0% lateral drift and ±2.5% lateral drifts, respectively. At east end, the buckled reinforcing bar fractured during the first cycle to +3.5% lateral drift. Subsequent reinforcing bars in the ends of the wall fractured during the next two cycles to +3.5% lateral drift. At west end, the localized lateral instability occurred in the end of the wall during the first cycle to +3.5% lateral drift. Vertical reinforcement fracture did not occur at the east end until the third cycle to -3.5% drift. The final condition on the east end of wall M2 is shown in Fig. 6-c.

The first flexural crack initiated during the first cycle to +0.2% lateral drift with a wall base moment of 294.6 kN-m, or roughly 43% of the peak strength. As shown in Fig. 8-c, the inelastic response of wall M2 was stable up until ±2.5% lateral drift when buckling of the vertical reinforcement occurred and caused a gradual degradation in wall strength. Three vertical reinforcing bars fractured during the second cycle to +3.5% lateral drift, leading a 20% drop of peak strength. The moment-displacement curve was fatter than that wall M1 due to the higher reinforcement ratio, indicating that more energy was dissipated during the test.

4. Discussion

The instrumentation used allowed both the global and local response of the test walls to be investigated. The recorded data is interpreted in the following sections in terms of deformation components, curvature distribution, plastic hinge length, reinforcement strains and reinforcement buckling. The figures are plotted and discussed up until 2.5% lateral drift as displacement gauges at the low part of the wall were compromised at 3.5% lateral drift due to bar buckling and fracture.

4.1 Deformation components

To investigate the deformation contributions of different sections of the wall panel, the wall was split into four components F1, F2, F3 and F4, as shown in Fig. 4. The flexural deformations were calculated by double-integrating the curvatures calculated from vertical displacement gauges along both wall edges assuming plane sections remain plane. The shear deformations were computed directly from the diagonal displacement gauges in accordance with the methods proposed by Hiraishi [12]. The contributions of the five displacement components during the first cycle to each lateral drift level for the three test walls are shown in Fig. 8. The summation of these five displacement components correlated well with the wall displacement measured directly using string-pot displacement gauges, with an error typically less than 5%.

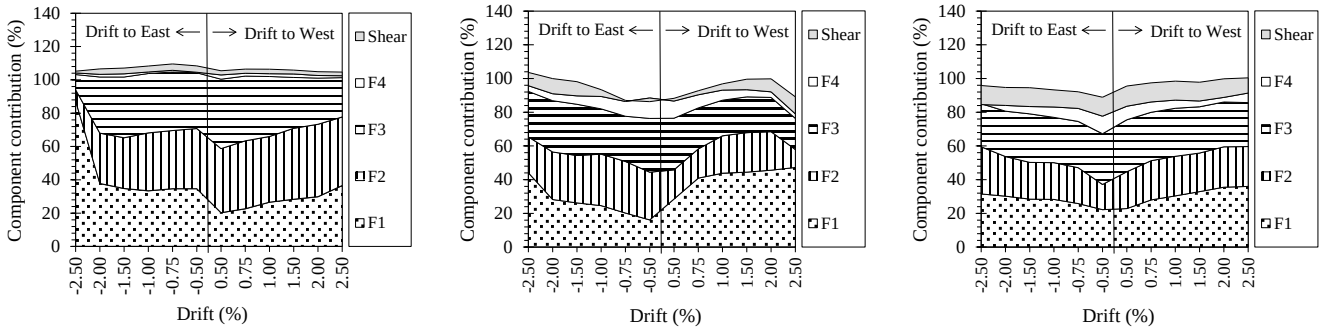

(a) Wall C6 (b) Wall M1 (c) Wall M2

Fig. 8 - Deformation components of the three test walls

For all the three walls, the flexural displacements were considerably larger than the shear displacements which roughly accounted for 5-12% of the total lateral displacement, confirming the walls was flexure dominant. Wall C6 was extremely flexure dominant and the shear deformations observed were significantly less than that recorded in the other two walls. For wall C6, component F1 that accounts for $1/14^{th}$ of the wall height contributed nearly 30-80% of the total lateral displacement in different drift levels. These local deformations confirmed that inelastic deformation was not distributed over a large length of the wall height, and that the wall behaviour was instead dominated by 2-3 main flexural cracks at the wall base. As the cracks in wall M1 and M2 were more evenly distributed over the plastic hinge region, the flexural deformation of were also more averagely distributed among the flexural panel regions up the wall height. Unlike wall C6, the three components F1, F2 and F3 of wall M1 and M2 were all roughly contributed 20-40% of the total lateral displacement. In addition, the component F4 of wall M1 and M2 contributed 5-10% of the total deformation while that of wall C6 nearly contributed 0. This confirmed that inelastic deformation was distributed over a large length of the wall height. The deformation components of M2 and M1 were similar to each other, except for a slightly larger contribution for shear in wall M2 due to the increased wall strength.

4.2 Curvature distribution

The average curvature distributions calculated from the displacement gauges up the wall height at the first cycle to each drift target for the three test walls are shown in Fig. 9. The curvature distributions further confirmed the observed wall behaviour and correlated well with the crack patterns shown in Fig. 5 and the deformation component shown in Fig. 8. For wall C6, the curvature distribution contained a few sharp peaks at the location of wide cracks as opposed to continuously distributed curvatures over the wall height, indicating the lateral deformation was concentrated at a few primary cracks at the wall base with limited secondary cracking. However, for wall M1 and M2, the curvatures were more continuously distributed over the wall height. The characteristic of this curvature distribution was also found in other ductile wall tests [13] and was typical of ductile RC members with a well distributed plastic hinge [14]. The curvature distribution of wall M2 were slightly more even and stable than that of wall M1 as there were more secondary cracks occurring over the wall height.

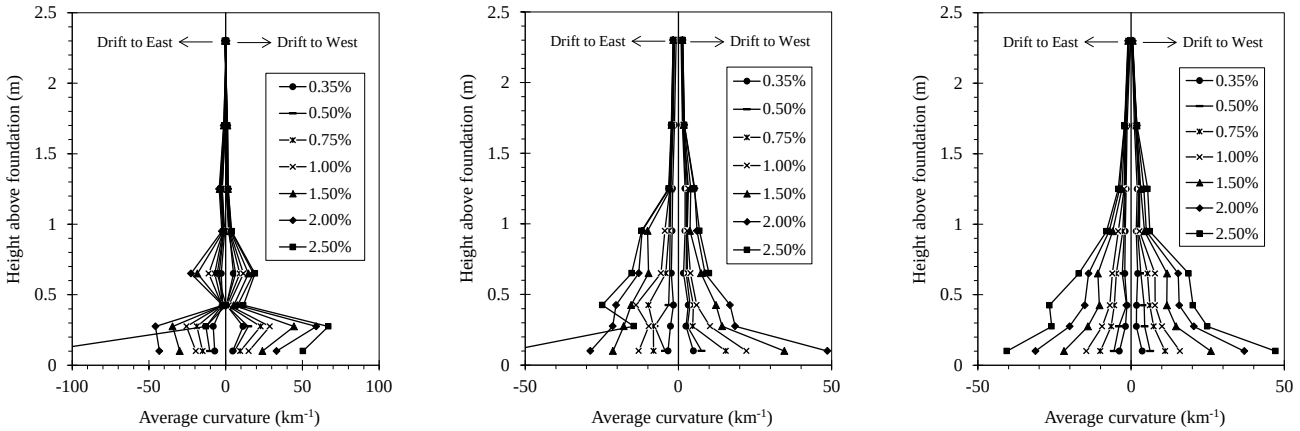

(a) Wall C6 (b) Wall M1 (c) Wall M2

Fig. 9 - Curvature distributions over the height

4.3 Plastic hinge length

The plastic rotation (θ_p) was calculated by integrating the plastic curvature profile over the entire wall height, where the yield curvature was defined as $\varphi_y = 2\varepsilon_y / l_w$ [15]. The equivalent plastic hinge length (l_p) was then calculated according to Eq. 3, where φ_m is the maximum curvature measured during the test.

$$\theta_p = \left(\varphi_m - \varphi_y\right) l_p \tag{3}$$

The plastic hinge length calculated at each drift cycle for each of the three test walls are plotted in Fig. 10 alongside the theoretical plastic hinge length calculated in accordance with NZS 3101 [9]. In NZS 3101 [9], the plastic hinge length is calculated as the smaller of $0.15M/V$ and $0.5l_w$, which is consistent with recommendations from previous researchers [16, 17]. The NZS 3101 plastic hinge length for the three walls with a shear span ratio of 4 was controlled by $0.5l_w$ (or 700 mm). The measured plastic hinge length in the positive and negative loading directions was not symmetrical due to the influence of different crack patterns. As shown in Fig. 10, the average plastic hinge length calculated from the test response for wall C6 was about 450 mm, below the theoretical plastic hinge length due to the concentrated inelastic behaviour at the wall base. However, for wall M1 and M2, the average plastic hinge length calculated from the test response was roughly equal to 725 mm and correlated well with the plastic hinge length assumed by NZS 3101. These results highlight that traditional assumptions for plastic hinge length analysis are not suitable for walls with lightly reinforced walls with a minimum required distributed vertical reinforcement, such as for NZS 3101:2006 (A2), but are applicable for the walls with additional vertical reinforcement in the ends of the wall to ensure secondary cracking, as per proposed requirements in NZS 3101:2006 (A3 draft).

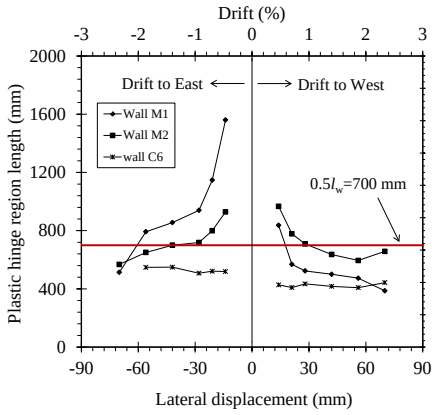

Fig. 10 - Calculated plastic hinge lengths

4.4 Reinforcement strains

The average tensile strains measured along the extreme vertical reinforcement up the height of the wall are plotted in Fig. 11 for each test wall.

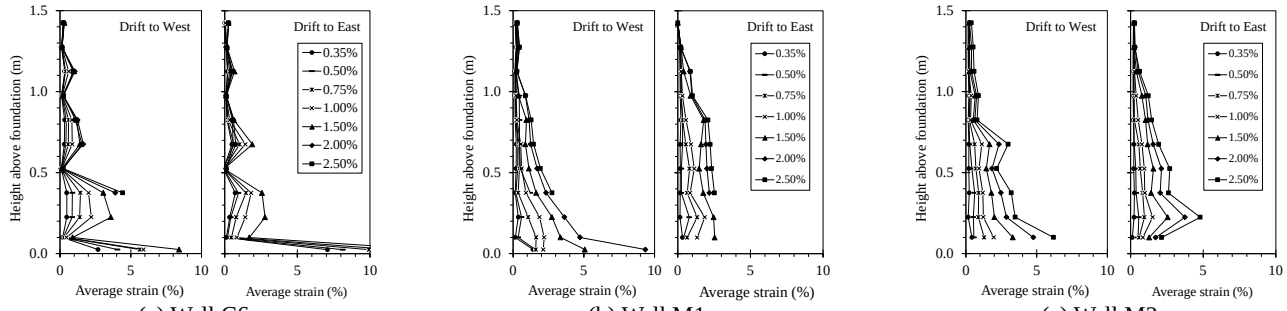

(a) Wall C6 (b) Wall M1 (c) Wall M2

Fig. 11 - Average strains along the corner vertical reinforcement

The strains were obtained by dividing the readings from the displacement gauges welded onto the vertical reinforcement as shown in Fig. 4 by the corresponding gauge length of 150 mm. Strains measurements were compromised after the reinforcement buckled and so these values are not plotted in Fig. 11. Unlike well detailed ductile RC walls where the reinforcement strains are evenly distributed over the plastic hinge length [13, 18], the reinforcement strains in wall C6 were inconsistent up the wall height with inelastic strains concentrated at crack locations. Large reinforcement strains occurred at the wall base, further confirming the concentrated inelastic deformations at 1-2 flexural cracks. For wall M1 and M2, the reinforcement strain distributed more evenly over the plastic hinge length which were similar with well detailed ductile RC walls [13, 18], indicating that

concentrating a greater portion of the reinforcement in the end of the wall can greatly improve the distribution of inelastic strains in lightly reinforced concrete walls. The reinforcement strain distributions for wall M1 and M2 were similar, indicating that increasing the reinforcement in the ends of the wall from 1.0% to 1.44 did not have a significant effect on the reinforcement strains.

4.5 Reinforcement buckling

As discussed earlier, the failure of all the three walls was controlled by buckling and subsequent fracture of the vertical reinforcement. Wall C2 were originally designed for limited ductility requirements in accordance with NZS 3101 [9] which currently states that anti-buckling reinforcement is only required when the vertical reinforcement ratio exceeds $3/f_y$ in limited ductile hinges or $2/f_y$ in ductile hinges (clause 11.4.6.3). The commentary to this clause explains that in the critical flexural compression zone of walls, reinforcement buckling and concrete spalling is not expected to occur if the vertical reinforcement ratio is low. Similar provisions can also be found in ACI 318-14 [5] which states that anti-buckling ties are only required when the vertical reinforcement ratio exceeds $2.76/f_y$. In the case of the test walls, anti-buckling ties were not required as the vertical reinforcement ratio of 0.53% was less than the limits in NZS 3101 [9] and ACI 318-14 [5]. However, even when D6@60 mm stirrups were placed in the toes of wall C6, which was compliant with current anti-buckling requirements of a ductile hinges in NZS 3101:2006 (A2), the vertical reinforcement still buckled at relatively modest lateral drifts of 1.5%. The wide cracks that form in lightly reinforced concrete walls increases the concentration of inelastic strains in the vertical reinforcement, resulting in a high chance of reinforcement buckling at moderate drifts. Furthermore, buckling initiates due to the large reinforcement tensile strains and transverse anti-buckling stirrups do not appear to be able to prevent this buckling.

As previously stated, the reinforcement buckling observed in wall M1 occurred during later drift cycles than wall C6, indicating that increasing the vertical reinforcement can delay reinforcement buckling. Increasing the vertical reinforcement resulted in an increased number of secondary cracks allowed the reinforcement strains to be more evenly distributed over the plastic hinge region. This even distribution of plasticity helped delay buckling of the vertical reinforcement by avoiding the large vertical reinforcement tensile strains that develop at wide concentrated cracks, as was the case for wall C6. Despite the cracking behaviour of wall M2 and M1 being similar, reinforcement buckling was delayed in wall M2 when compared to wall M1. It appears that the stability of the larger diameter reinforcing bars in wall M2 helped further delay the initiation of reinforcement buckling.

5. Conclusions

The test results of three lightly reinforced concrete walls designed in accordance with the minimum vertical reinforcement requirements in NZS 3101:2006 (amendment 2 and amendment 3) were presented. The test observations and results including crack pattern, failure mode and overall hysteric response were presented and test response was discussed in terms of deformation components, curvature distribution, plastic hinge length, reinforcement strains and reinforcement buckling. The main conclusions drawn from this experimental study are summarized as follows:

- The behaviour of wall C6 with minimum distributed reinforcement in accordance with NZS 3101:2006 (A2) was controlled by 3-4 large flexural cracks at the wall base.
- The increased vertical reinforcement in the ends of walls M1 and M2 in accordance with NZS 3101:2006 (A3 draft) resulted in a significant increase in the number and distribution of cracks in the plastic hinge region.
- Traditional assumptions for plastic hinge length analysis are not suitable for lightly reinforced walls with a minimum required distributed vertical reinforcement, such as for NZS 3101:2006 (A2), but are applicable for the walls with additional vertical reinforcement in the ends of the wall that ensure secondary cracking.
- Increasing the vertical reinforcement content in the ends of the wall delay the onset of reinforcement buckling due to the reinforcement strains being more evenly distributed over the plastic hinge region.

6. Acknowledgements

The authors would like to acknowledge the funding provided by the Natural Hazards Research Platform, China Scholarship Council (CSC), and the Building Performance Branch of the Ministry of Business, Employment and Innovation (MBIE), in addition to project support and management provided by the UC Quake Center.

7. References

[1]. Structural Engineering Society of New Zealand (SESOC), Preliminary observations from Christchurch earthquakes, Report prepared for the Canturbury Earthquakes Royal Commission http://canterbury.royalcommission.govt.nz/documents-by-key/20111205.1533.2011.

[2]. Kam, W Y, S Pampanin, and K J Elwood (2011), Seismic performance of reinforced concrete buildings in the 22 Feburary Christchurch (Lyttelton) earthquake. *Bulletin of the New Zealand Society for Earthquake Engineering*, 44 (4), 239-278.

[3]. Sritharan, S, K Beyer, R S Henry, Y H Chai, M Kowalsky, and D Bull (2014), Understanding poor seismic performance of concrete walls and design implications. *Earthquake Spectra*, 30 (1), 307-334.

[4]. Henry, R S (2013), Assessment of minimum vertical reinforcement limits for RC walls. *Bulletin of the New Zealand Society for Earthquake Engineering*, 46 (2), 88-96.

[5]. ACI 318-14, Building Code Requirements for Structural Concrete (ACI 318-14) and Commentary, American Concrete Institute: Farmington Hills, Michigan.2014.

[6]. CEN, Eurocode 8: Design of structures for earthquake resistance, European Committee for Standardization: Brussels, Belgium.2004.

[7]. CSA, Design of concrete structures. Standard CSA-A23.3-14, Canadian Standards Association: Toronto.2014.

[8]. GB 50010-2010, Code for design of concrete structures China Architecture&Building Press: Beijing.2010.

[9]. NZS 3101:2006, Concrete Structures Standard (Amendment 2), Standards New Zealand: Wellington, New Zealand.2006.

[10]. NZS 3101:2006, Concrete Structures Standard (Amendment 3 - Draft), Standards New Zealand: Wellington, New Zealand.2015.

[11]. Russell, A, R S Henry, and R C Fenwick, Design of RC walls post the Canterbury earthquakes, in *Proceedings of the Concrete Industries Conference*: Rotorua.2015.

[12]. Hiraishi, H (1984), EVALUATION OF SHEAR AND FLEXURAL DEFORMATIONS OF FLEXURAL TYPE SHEAR WALLS. *Bulletin of the New Zealand National Society for Earthquake Engineering*, 17 (2), 135-144.

[13]. Dazio, A, K Beyer, and H Bachmann (2009), Quasi-static cyclic tests and plastic hinge analysis of RC structural walls. *Engineering Structures*, 31 (7), 1556-1571.

[14]. Paulay, T and M J N Priestley, Seismic design of reinforced concrete and masonry buildings. New York: New York : Wiley c1992.1992.

[15]. Priestley, M J N and M J Kowalsky (1998), Aspects of drift and ductility capacity of rectangular cantilever structural walls. *Bulletin of the New Zealand National Society for Earthquake Engineering*, 31 (2), 73-85.

[16]. Wallace, J W and K Orakcal (2002), ACI 318-99 provisions for seismic design of structural walls. *ACI Structural Journal*, 99 (4), 499-508.

[17]. Adebar, P, J Mutrie, and R DeVall (2005), Ductility of concrete walls: The Canadian seismic design provisions 1984 to 2004. *Canadian Journal of Civil Engineering*, 32 (6), 1124-1137.

[18]. Adebar, P, A M M Ibrahim, and M Bryson (2008), Test of high-rise core wall: Effective stiffness for seismic analysis. *ACI Structural Journal*, 105 (4), 509-512.